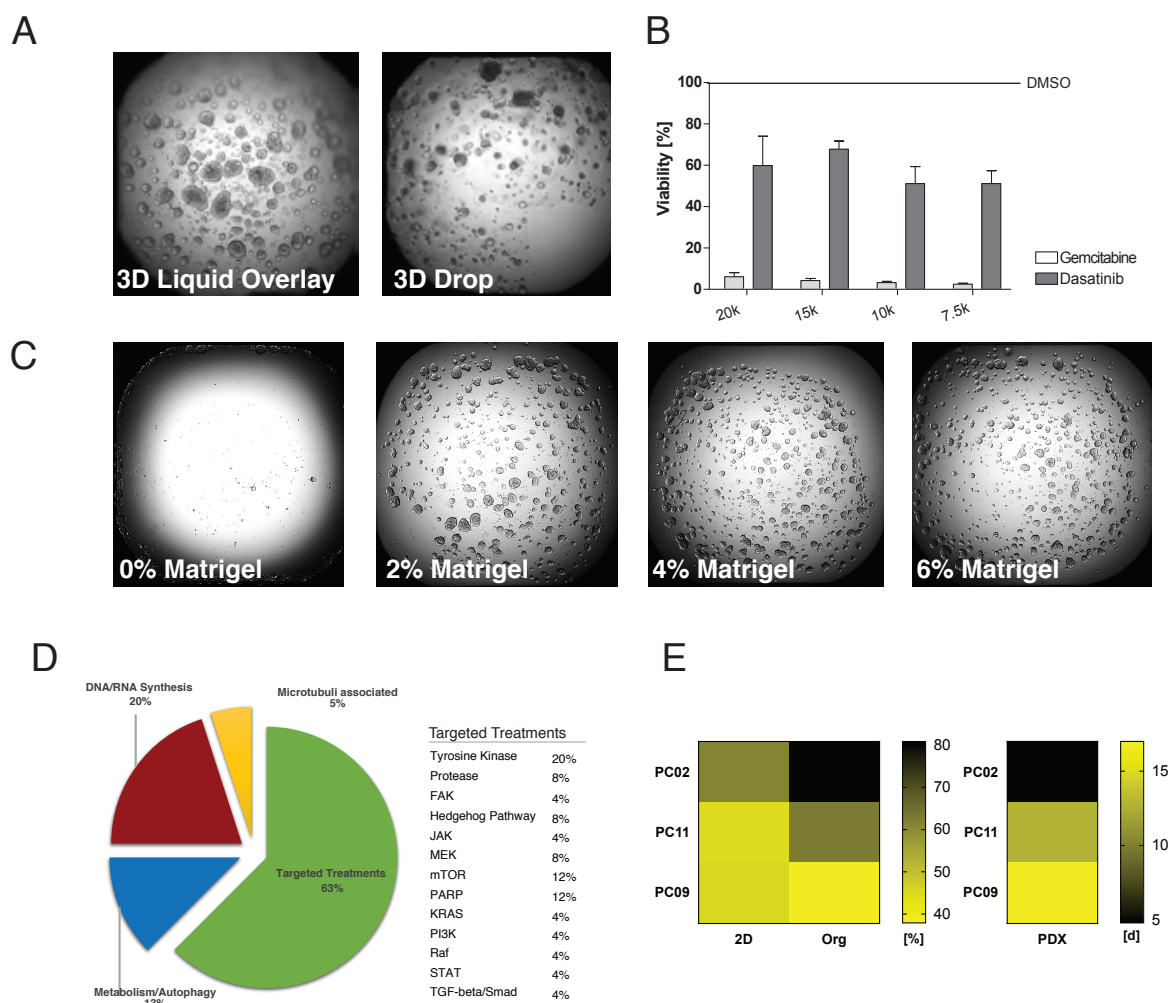
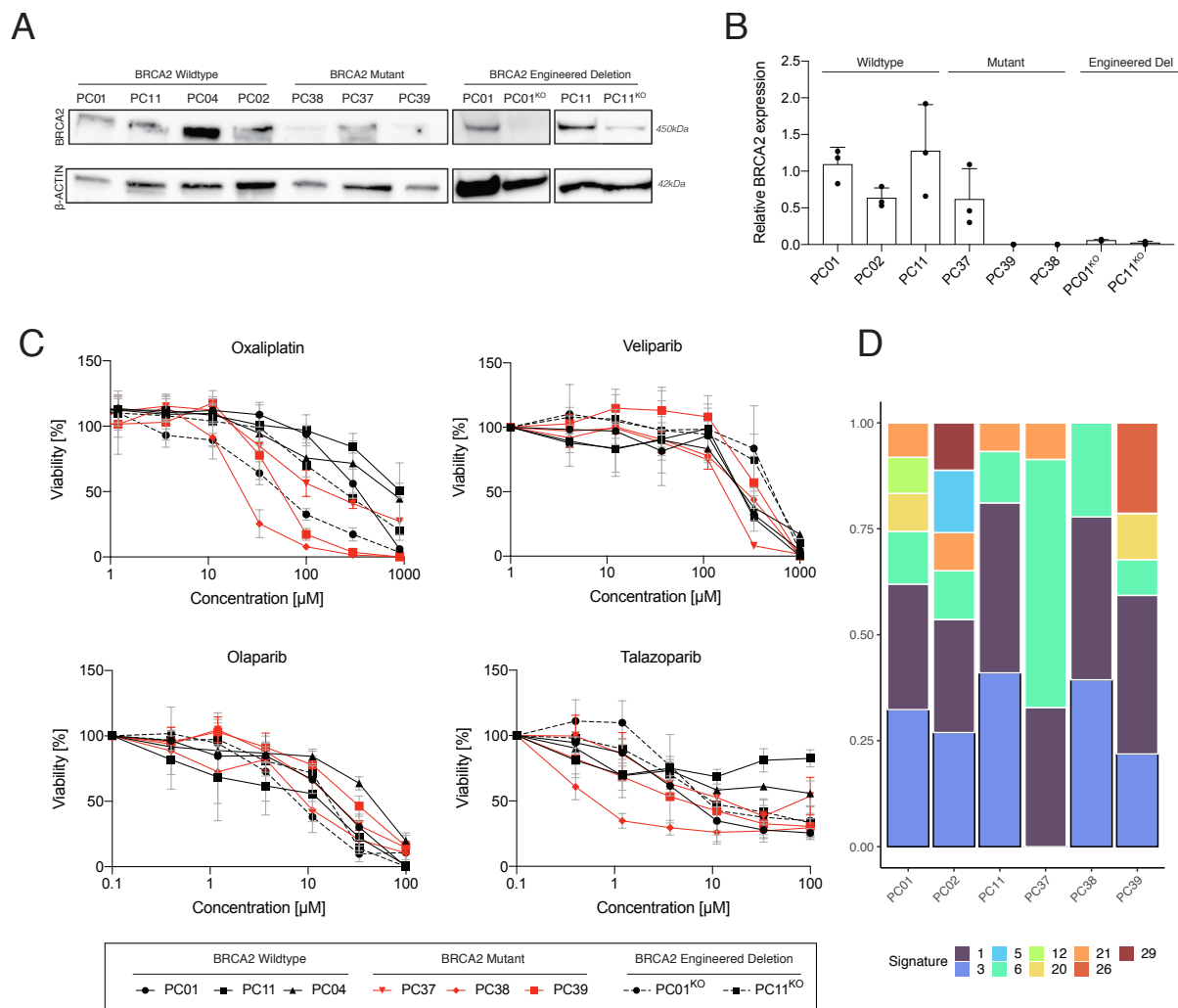


**Figure S1. *In vivo* PDAC phenotypes correlate with *in vitro* PDAC organoid phenotypes, Related to Figure 1. (A)** Phenotype of primary PDAC patient tissues (H&E), of corresponding PDAC organoids *in vitro* (brightfield image), and after subcutaneous transplantation of organoids into mice (H&E). Scale bar 100 $\mu$ m. **(B)** Phenotype of PDAC PDX tissues (H&E), of corresponding PDAC organoids *in vitro* (brightfield image), and after subcutaneous re-transplantation of organoids into mice (H&E). Organoids were passaged >5 times before re-transplantation. Scale bar 100 $\mu$ m. **(C)** Initial tumor growth of PDX lines (PDX 1 & 2 indicates two different PDX lines established from the same initial tumor), and tumor growth of re-transplanted lines after *in vitro* expansion as organoids (blue). Organoids were passaged >5 times before re-transplantation.



**Figure S2. Establishment of a drug screening platform for PDAC organoids, Related to Figure 2.**

(A) Brightfield image of the PC02 organoid line in a 3D drug liquid overlay organoid culture and a standard drop organoid culture (Matrigel dome). (B) Seeding of different cell numbers and influence on the drug response. Viability was calculated by normalizing each dose to the DMSO treated control. Gemcitabine and Dasatinib at a reference dose of  $1\mu\text{M}$ . Data is represented as means  $\pm$  SDs based on technical and biological replicates. (C) Effect of matrigel supplementation in organoid growth medium in the 3D drug liquid overlay culture system – representative brightfield images. (D) The PDAC compound library was composed of drugs approved for PDAC treatment or currently tested in clinical trials. 20% of compounds target the DNA/RNA synthesis pathway, 5% the microtubule-associated pathway, 13% are metabolism/autophagy related, and 62% target other tumor-related signaling pathways. (E) Drug responses for erlotinib in corresponding 2D monolayer-, 3D organoid-, and PDX lines. *In vitro* drug response shown as % viability at a dose of  $10\mu\text{M}$ , *in vivo* drug response shown as days to reach 200% tumor volume.



**Figure S3. Correlating *BRCA2* mutations with PARPi response in PDAC organoids, Related to Figure 3.** (A) Western blot showing *BRCA2* and  $\beta$ -ACTIN protein expression. (B) *BRCA2* mRNA expression assessed by qRTPCR.  $n = 3$  independent biological replicates. Loss of gene expression in PC38 and PC39 suggest silencing of the WT allele. As PC39 carries a missense mutation in *BRCA2*, we speculate that this mutation leads to aberrant splicing, a phenomenon that is frequently observed for SNVs in *BRCA1/2*<sup>67</sup>. (C) Response profile of genuine *BRCA2*-mutant organoids (red), *BRCA2*-WT organoids (black) and CRISPR-Cas9 engineered *BRCA2*-mutant organoids (dashed lines) to oxaliplatin and to the different PARP-inhibitors veliparib, olaparib, and talazoparib. Viability was normalized to solvent control (0.1% DMSO or 0.1% ddH<sub>2</sub>O). Data is represented as means  $\pm$  SDs based on technical and biological replicates. (D) Relative contribution of COSMIC mutation signatures in PDAC samples.

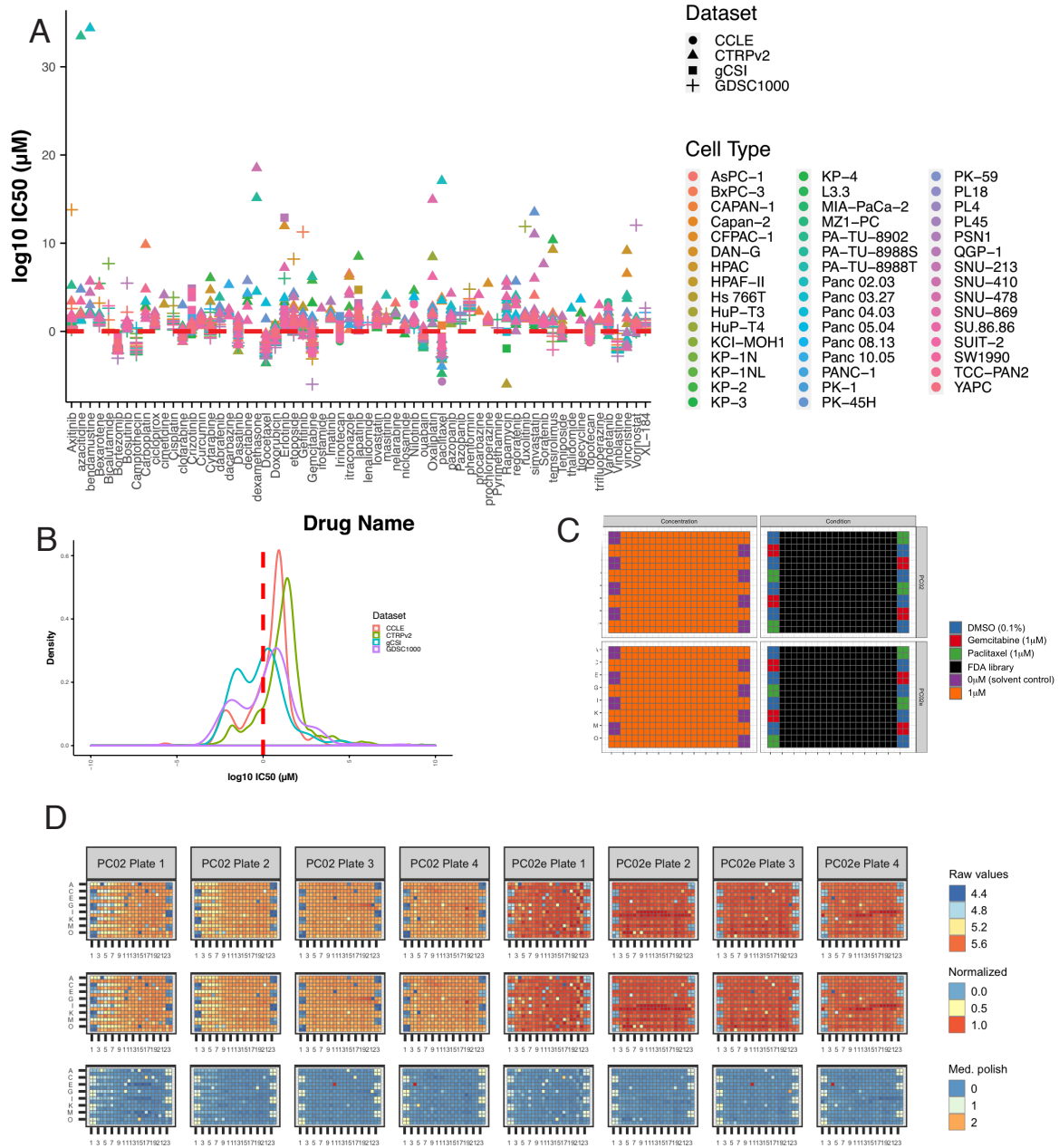


**Figure S4. Reported IC<sub>50</sub> values of FDA-approved compounds in PDAC cell lines and floor plan of the high-throughput screen, Related to Figure 4.** (A) Single IC<sub>50</sub> values of 63 FDA-approved compounds in different PDAC cell lines. All compounds shown here were present in our drug library. Dashed red line corresponds to the chosen screening dose (1µM) in this study. Data was obtained from PharmacDB. (B) Combined IC<sub>50</sub> values of the 63 compounds shown in A. Dashed red line corresponds to the chosen screening dose (1µM) in this study. Data was obtained from PharmacDB. (C) Layout of the automated high-throughput screen in the 384-well format showing location of controls and compounds. (D) Raw (top) and normalized (center) values of the different screening plates for both organoid lines (PC02 and PC02e). To remove spatial effects over the plates, we performed Tukey's median polish procedure (Tukey, 1977) prior to hit selection (bottom).

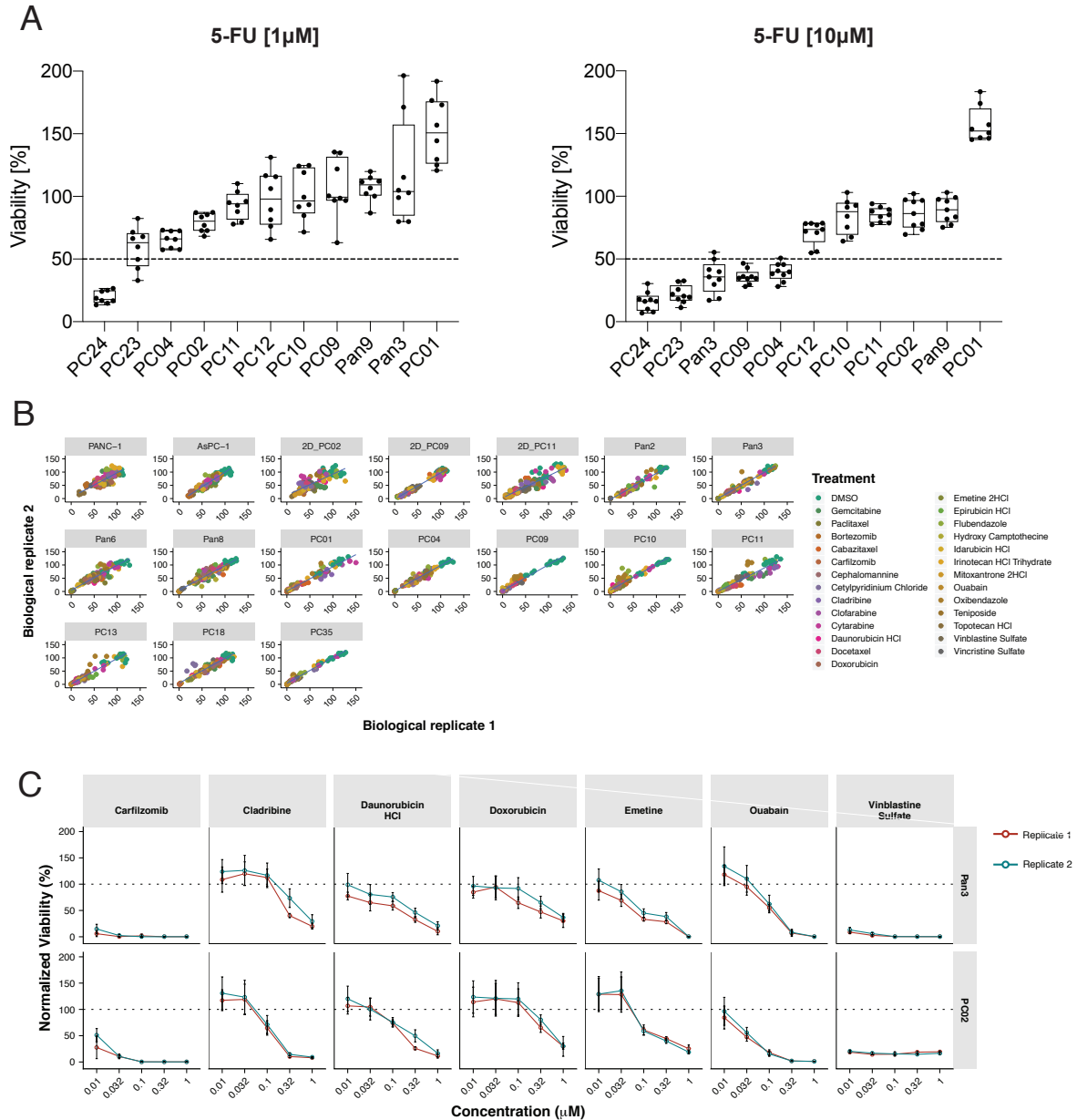


**Figure S5. Quality values of automation for drug screening and validation screens, Related to Figure 5.** (A) 5-FU treatment in PDAC and WT organoid lines at indicated dosages. Technical replicates of two independent experiments are shown as Tukey plots. (B) Correlation of the two different biological replicates summarized in the heatmap presented in Figure 5A. (C) Response-profiles of hits selected for *in vivo* validation visualized in normalized values over a 5-fold dose-range. Biological replicate 1 shown in red, biological replicate 2 shown in blue. Data is represented as means  $\pm$  SDs based on technical replicates.

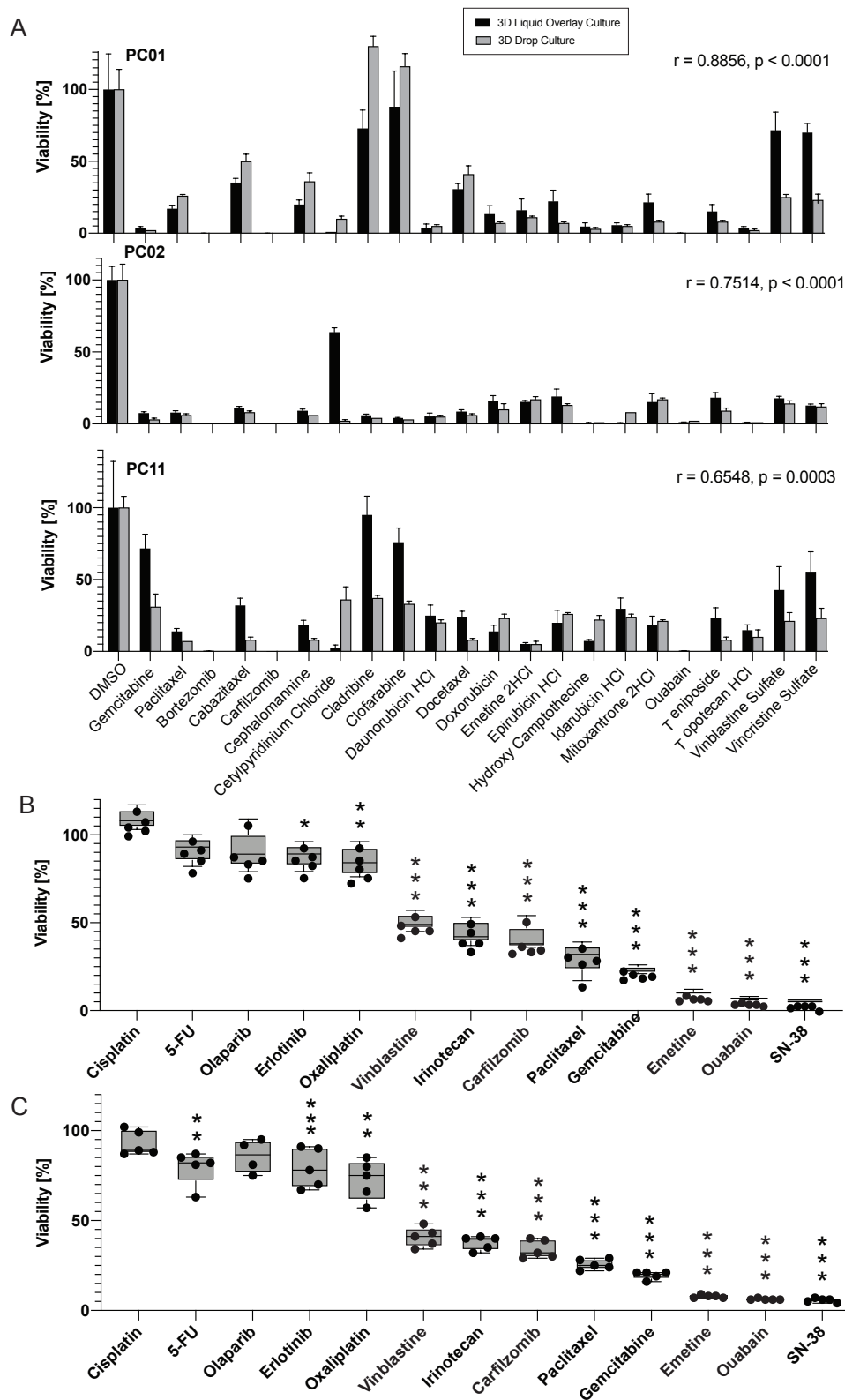


**Figure S6. Confirmation of screening hits in PDAC organoids grown in conventional 3D Matrigel domes and metastatic PDAC organoids, Related to Figure 5. (A)** Viability in 3D liquid culture overlay assays and 3D Matrigel dome cultures in three organoid lines. Viability was normalized to solvent control (0.1% DMSO). Data is represented as means  $\pm$  SDs based on technical and biological replicates at a reference dose of  $1\mu\text{M}$  for each compound.  $r$  = Pearson correlation analysis. **(B-C)** Viability of two metastatic PDAC organoid lines treated with  $1\mu\text{M}$  of each compound. Viability was normalized to solvent control (0.1% DMSO). Data is represented as box plots based on technical and biological replicates. \* $<0.05$ , \*\* $<0.01$ , \*\*\* $<0.001$ ; one-way ANOVA with Dunnett post-hoc test.

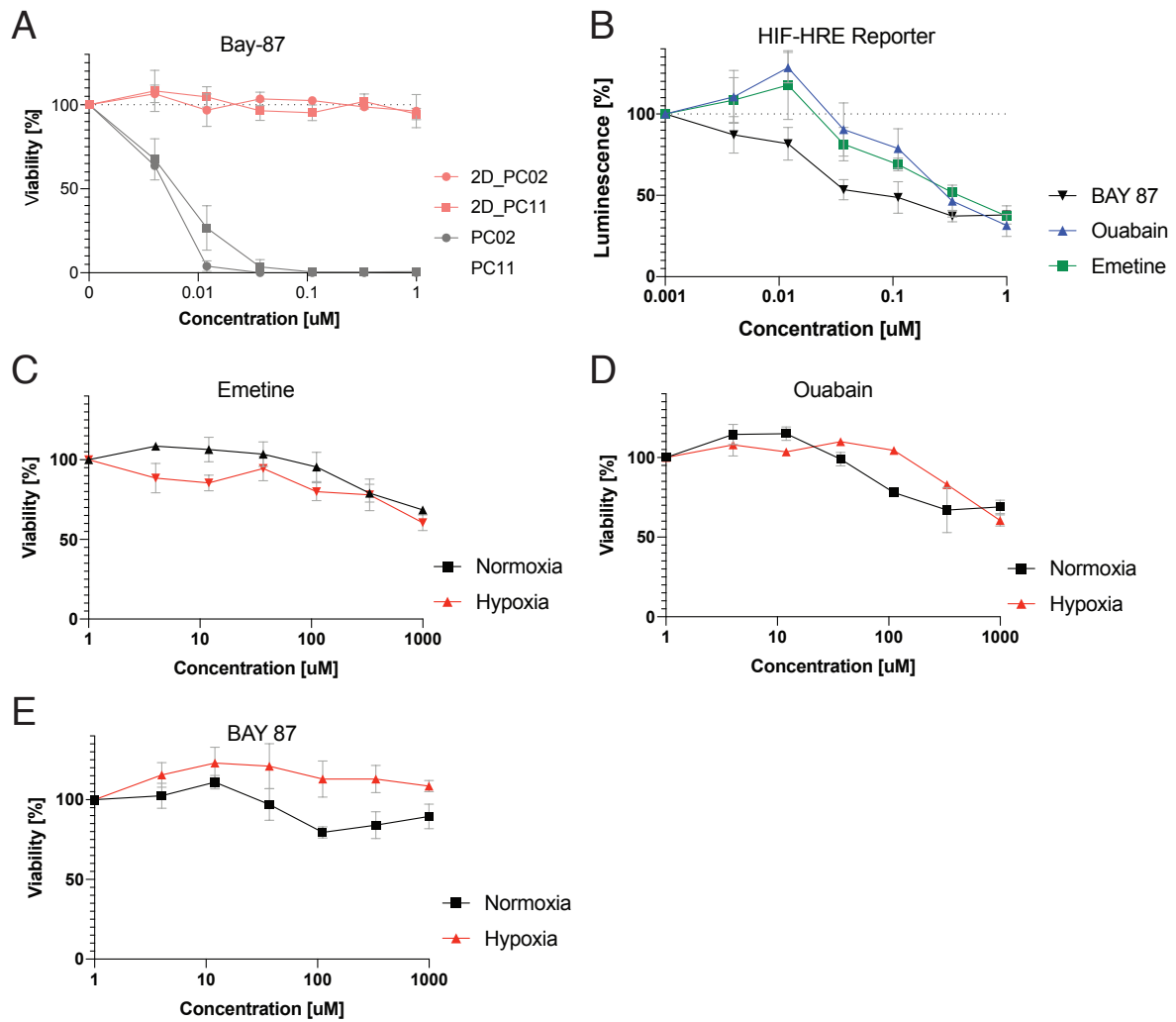


**Figure S7. Effect of HIF inhibitors on PDAC monolayer cultures, Related to Figure 6.**

(A) Response profile of isogenic 2D monolayer and 3D organoid PDAC lines to the HIF-inhibitor BAY-87. Viability was normalized to solvent control (0.1% DMSO). Data is represented as means  $\pm$  SDs based on technical and biological replicates. (B) Effect of emetine, ouabain and BAY 87 on HIF-HRE reporter activity. The reporter was stably integrated in PANC1 cell lines. Cells were grown under 1% O<sub>2</sub> hypoxia. Luminescence was normalized to solvent control (0.1% DMSO). Data is represented as means  $\pm$  SDs based on technical and biological replicates. (C-E) Survival response of PANC1 cells to emetine, ouabain and BAY 87 grown under normoxia (black) and 1% O<sub>2</sub> hypoxia (red). Viability was normalized to solvent control (0.1% DMSO). Data is represented as means  $\pm$  SDs based on technical and biological replicates.